Wetting Dynamics in a Confined Symmetric Binary Mixture Undergoing Phase Separation

Hajime Tanaka
Institute of Industrial Science, University of Tokyo, Minato-ku, Tokyo 106, Japan
(Received 29 December 1992)

Here we study the interplay between wetting and phase separation for a nearly symmetric binary mixture confined in a one-dimensional (1D) or a two-dimensional (2D) capillary. It is found that near the symmetric composition, the hydrodynamics unique to bicontinuous phase separation plays a crucial role in the wetting dynamics and the surface effect is strongly delocalized by the interconnectivity of the phases. The growth rate of the wetting droplet and the thickening rate of the wetting layer are discussed on the basis of the hydrodynamic coarsening. The effect of the dimensionality of the geometrical confinement is also discussed.

PACS numbers: 64.75.+g, 05.70.Fh, 64.60.-i, 68.45.Gd

Phase separation phenomena have been extensively studied in the past two decades from both the experimental and the theoretical viewpoints [1]. Since the finding of critical wetting phenomena by Cahn [2], static wetting phenomena have been widely studied in the stable region [3–7]. Both phenomena have long histories of research, but they have been studied almost independently. However, because both phase separation and critical wetting occur near the criticality, these two nonequilibrium phenomena can be coupled with each other. From this standpoint, much attention has recently been paid to the interplay between phase separation and wetting in the unstable or metastable states, and it has been revealed that phase separation can be strongly affected by wetting phenomena in a confined geometry [8–14]. Phase separation creates two semimacroscopic phases having different wettability, and the wettability causes the interaction between the phases and the solid surface. Thus the phases are spatially rearranged to lower the total energy including the solid-liquid interactions. The late stage of pattern evolution is governed by the competition between the liquid-liquid and solid-liquid interfacial energies. Since wetting dynamics is coupled with phase separation in complicated manners, the coarsening dynamics under the influence of wetting has not been clarified yet. Wetting dynamics could be strongly dependent on the type of bulk phase separation. In droplet phase separation, droplets gradually wet to the walls and slowly form the wetting layer [14]. In bicontinuous phase separation, on the other hand, the wetting dynamics is found to be very different from that in droplet phase separation because of the interconnectivity of the phases. In this Letter, we discuss the wetting dynamics of a nearly symmetric mixture undergoing phase separation in a one-dimensional (1D) or a two-dimensional (2D) capillary, focusing on the effects of the kind of geometrical constraint on the pattern evolution.

The samples used were the mixtures of poly(vinyl methyl ether) (PVME) and water and the mixtures of ϵ-caprolactone oligomer (OCL) and styrene oligomer (OS). The weight-average molecular weight M_w of PVME was 98 200. The M_w of OCL and OS was 2000 and 1000, respectively. In PVME/water mixtures, the water-rich phase is more wettable to glass than the PVME-rich phase. In OCL/OS mixtures, the OCL-rich phase is more wettable to glass than the OS-rich phase. A sample mixture was set in a 1D capillary with the inner tube radius of r_0 or in a 2D capillary composed of two parallel plates with a gap of d. d was controlled by using monodisperse glass beads. Phase separation was triggered by a temperature jump from the stable, one-phase region to the unstable, two-phase region with a rate of 1.5 °C/s. The temperature of the sample was changed by using a hot stage (Linkam TH-600RMS). We directly observed the pattern evolution dynamics with video optical microscopy.

Figure 1 shows the pattern evolution of the PVME/water (7/93) (weight ratio) mixture confined in a 1D capillary (r_0 = 79 μm) at 33.3 °C. The phase separation temperature was 33.1 °C. Since this composition was symmetric, bicontinuous phase separation was observed

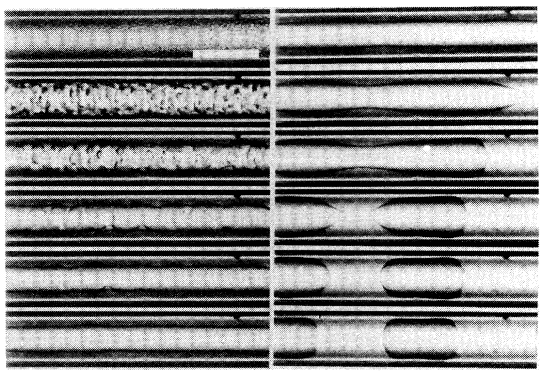

FIG. 1. Phase separation of PVME/water (7/93) in a 1D capillary. Photographs correspond to 0.5 s, 1.5 s, 2.5 s, 3.5 s, 4.5 s, 8.5 s (left column), 58.5 s, 148.5 s, 178.5 s, 238.5 s, 246.5 s, and 268.5 s (right column) from top to bottom, respectively, after the temperature jump from 32.5 °C to 33.3 °C. The bar is 200 μm in length.

in the initial stage. Then the macroscopic wetting layer was rapidly formed. After the formation of the wetting layer, the Rayleigh instability led to the formation of bridges [14]. Figure 2 shows the pattern evolution of the PVME/water (7/93) mixture confined in a 2D capillary ($d \sim 19$ μm) at 33.7 °C. In the initial stage, the bicontinuous pattern was observed [see (a) and (b)]. Then, the wetting layer formation and the subsequent formation of disklike droplets from the tubes bridging the upper and lower plates were observed [see (c) and (d)]. The latter is unique to a 2D system. In the late stage, the disklike droplets were attracted to each other by the wetting-induced interaction due to the capillary instability [see (e) and (f)]. After this stage the droplet pattern finally transformed into the bicontinuous pattern because of an increase in the apparent in-plane symmetry reflecting the thinning of the wetting layer [14]. Very similar behavior was observed for both PVME/water (7/93) and OCL/OS (3/7) mixtures confined in a 2D capillary for various quench conditions and various sample thicknesses. It should be noted that this wetting-induced pattern formation was unique to nearly symmetric compositions and it was never observed in asymmetric compositions, where droplet phase separation occurs. In the latter, droplets gradually wet to the walls and the wetting speed is much slower than in bicontinuous phase separation.

Here we discuss the composition effects on the wetting behavior and the final wetting-induced morphology. The obvious dependence on the composition comes from the difference in the morphology of the bulk phase separation, namely, whether the bulk phase separation is bicontinuous type or droplet type. This mainly affects

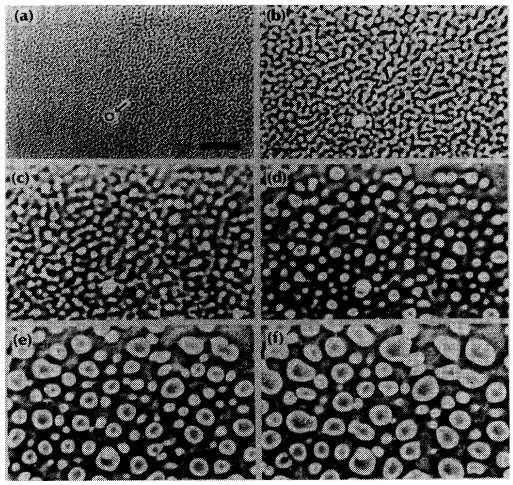

FIG. 2. Phase separation of PVME/water (7/93) in a 2D capillary ($d = 19$ μm). (a) 0.7 s, (b) 1.7 s, (c) 2.2 s, (d) 2.7 s, (e) 3.7 s, and (f) 4.7 s after the temperature jump from 32.8 °C to 33.7 °C. The arrow in (a) indicates the glass bead with the diameter of 19 μm. Its real size is also drawn in (a). The bar is 100 μm in length.

the wetting dynamics. Another important factor is the composition effect on the final equilibrium configuration under the influence of the wetting effect.

First we consider the composition effects on the final equilibrium configuration for a thin 2D capillary. In the late stage of phase separation, we need consider only the free energy originating from the interface. There are two possible final configurations: (1) layer structure (complete wetting configuration) and (2) disklike droplet structure (partial wetting configuration). The free energies per unit area for the configurations of complete and partial wetting are given by $F_{\rm cw} = 2(\gamma_\alpha + \sigma)$ and $F_{\rm pw} = 2\phi_\alpha\gamma_\alpha + 2\phi_\beta\gamma_\beta + \sigma f(d)$, respectively. σ is the interfacial tension between the α and β phases and γ_i is the interfacial tension between the i phase and the wall. ϕ_α and ϕ_β are the volume fraction of the α and β phases, respectively. Here the α phase is more wettable to the wall. $f(d)$ is the total interface area between the α and β phases per unit area. Neglecting the last term in $F_{\rm pw}$, $F_{\rm cw} - F_{\rm pw} = 2\sigma(1 - \phi_\beta\Delta\gamma/\sigma)$, where $\Delta\gamma = \gamma_\beta - \gamma_\alpha$. The morphological transition occurs at $\phi_\beta = \sigma/\Delta\gamma$.

Next we consider the equilibrium configuration for a 1D capillary. As discussed by Liu *et al.* [9], the free energies per unit length for the configurations of complete and partial wetting (*tube* and *plug*) for a 1D capillary are given by $F_{\rm cw}/2\pi = r_c\sigma + r_0\gamma_\alpha$ and $F_{\rm pw}/2\pi = r_0[\phi_\alpha\gamma_\alpha + \phi_\beta\gamma_\beta] + g(r_0)\sigma$, respectively. Here r_c is the radius of the fluid *tube* for the complete wetting configuration and $r_c^2 = \phi_\beta r_0^2$. $g(r_0)$ is the total interface area between the α and β phases per unit length for the partial wetting configuration. Provided that the last term in $F_{\rm pw}$ is negligible, $(F_{\rm cw} - F_{\rm pw})/2\pi = r_0\sigma[\phi_\beta^{1/2} - (\Delta\gamma/\sigma)\phi_\beta]$. The transition between the complete and partial wetting configurations occurs at $\phi_\beta = (\sigma/\Delta\gamma)^2$.

Since $\sigma = \sigma_0\epsilon^\mu$ ($\mu = 1.26$) and $\Delta\gamma = \Delta\gamma_0\epsilon^\delta$ ($\delta = 0.34$) where $\epsilon = (T - T_c)/T_c$, the transition compositions are given by $\phi_t = (\sigma_0/\Delta\gamma_0)\epsilon^{(\mu-\delta)}$ for a 2D capillary and by $\phi_t = (\sigma_0/\Delta\gamma_0)^2\epsilon^{2(\mu-\delta)}$ for a 1D capillary. Thus for both 1D and 2D capillaries, the partial wetting configuration is energetically favored near the symmetric composition except for a very shallow quench. This is consistent with our observation. The next problem is to clarify how the phase-separation pattern transforms from the initial, 3D bicontinuous pattern to the above final, equilibrium configuration.

Before discussing the pattern formation dynamics, we discuss a characteristic feature of bicontinuous phase separation near the symmetric composition. In this particular type of phase separation, the hydrodynamics due to the capillary instability [10,15] plays a drastic role in the coarsening under the influence of wetting. Near the symmetric composition, the wettability is probably important mainly in the initial stage to establish the initial condition that the surface is covered by the wetting layer, to which the bicontinuous tubes are connected. This initial configuration strongly affects the subsequent coars-

ening dynamics: It establishes the anisotropic pressure gradient from the bicontinuous tubes in bulk to the wetting layer and the more wettable phase can be continuously supplied into the wetting layer through the percolated tubes. This coarsening mechanism continues until the tube network disappears and the system completely separates into the two macroscopic phases. Because of the percolated structure, the wetting effect is not localized near the wall and strongly affects the whole sample (see Fig. 1). Thus, phase separation could be seriously affected by wetting phenomena especially near the symmetric composition even though a sample size is macroscopic. Further, the strong coupling between the concentration and the velocity fields and the resulting *interface quench effect* (the quick reduction of the interfacial energy) could cause double phase separation for a deep quench in bicontinuous phase separation [14].

Here we discuss the initial stage of the wetting droplet formation. This problem was experimentally studied in a 2D capillary by Wiltzius and Cumming [11]. They found that the size of the wetting droplet l grows as $t^{3/2}$ although the growth mechanism was not clear. In our experiments the quench depth was too deep to see this initial stage of the wetting layer formation. The anomalous, fast growth mode found by them could be explained as follows. There is a pressure gradient between a bicontinuous tube and its wetting part, reflecting the difference in the transverse curvature of the tube between them. Thus there should be a hydrodynamic flow from the tube to the wetting droplet. Since the pressure gradient between the tube and the wetting layer is $\sim \sigma/a$ over the distance a, the flux of this flow is estimated as $Q \sim (\sigma/\eta)a^2$, where η is the viscosity and a is the characteristic size of the tube. Provided that the limiting process of the droplet spreading is the supply of the more wettable phase from the tubes by the hydrodynamic flow, we get the relation $ldl/dt \sim Q$. The assumption is probably valid for the case of *strong wettability* and it is supported by the 2D nature of the droplet growth experimentally confirmed [11]. Using Siggia's growth law, $a \propto (\sigma/\eta)t$, we obtain the relation $l \sim [(\sigma/\eta)t]^{3/2}$. This is consistent with their observation. The prefactor $(\sigma/\eta)^{3/2}$ is roughly proportional to $(\Delta T)^{3\nu}$, where ΔT is the quench depth, ν is the critical exponent for the correlation length ξ, and $\nu \sim 0.63$. This dependence of the prefactor on ΔT seems to be consistent with the experimental results [11].

Next we discuss the thickening dynamics of the wetting layer. For both 1D and 2D capillaries, the thickening rate of the wetting layer $(d/dt)d_w$ should be proportional to the flux from the bicontinuous tubes after the formation of the wetting layer. It should be noted that for a 2D capillary, the present discussion is limited to the complete wetting case. The flux from a single tube Q can be estimated as $Q \sim (\sigma/\eta)a^2$ as before. The number of tubes per area S is proportional to S/a^2. Thus the total flux Q_t is proportional to $S(\sigma/\eta)$. Since the thickening of the wetting layer is caused by this flux, $S(d/dt)d_w \sim S(\sigma/\eta)$.

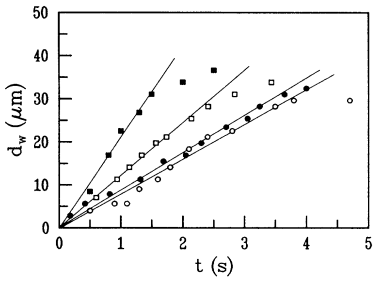

FIG. 3. Dynamics of wetting layer formation for PVME/water (7/93) in a 1D capillary. d_w is plotted against t. ○: 33.2 °C ($r_0 = 70.5$ μm); •: 33.4 °C ($r_0 = 98.7$ μm); □: 33.5 °C ($r_0 = 81.8$ μm); ■: 34.0 °C ($r_0 = 70.5$ μm).

Therefore, $d_w = k_w(\sigma/\eta)t$, where k_w is the proportional constant. This linear-growth behavior has been experimentally confirmed for 1D capillaries as shown in Fig. 3. The increase in the slope with an increase of the quench depth can be explained by the increase in σ. Thus the characteristic time (τ_w) required to form a macroscopically separated wetting phase having a size of d_c can be estimated as $d_c\eta/k_w\sigma$. Here $d_c = d\phi_\alpha$ (ϕ_α: the volume fraction of the more wettable phase) for a 2D capillary, and $d_c = r_0[1 - (1 - \phi_\alpha)^{1/2}]$ for a 1D capillary.

For both 1D and 2D capillaries, the wetting layer is formed from a bicontinuous, phase-separated structure. However, it should be noted that there is a striking difference in the late stage of pattern evolution between 1D and 2D capillaries as can be seen in Figs. 1 and 2. For a 1D capillary, the tube radius of the bicontinuous pattern a can never exceed the capillary tube radius r_0 because of the geometrical constraint. Thus the complete layer configuration is first formed and then the Rayleigh instability causes a stable bridge structure [14]. This instability is a result of the competition between the destabilizing effect of the transverse curvature at long wavelengths and the stabilizing effect of the longitudinal curvature at short wavelengths. The van der Waals interaction is another stabilizing factor [9], but should be weak in our case. This instability is characteristic of a 1D capillary. There is no analogous instability in a 2D capillary since the area of planar interface can only be increased by small perturbations. In a 2D capillary, on the other hand, the tube diameter $2a$ can exceed the spacing d since there is no geometrical restriction parallel to the plates. Once $2a$ becomes larger than d, the longitudinal curvature of the tube ($\sim 2/d$) becomes larger than its transverse curvature ($\sim 1/a$). Thus the pressure in the tube becomes lower than the wetting layer. Therefore, the tube bridging the two walls, having a radius of a ($> d/2$), starts to thicken with time by absorbing the wetting layers. This process can be seen in Fig. 2. Actually, we have found that the 2D disklike droplet appearing in a 2D capillary always has the initial diameter $2a_0$ comparable to the thickness d as shown in Fig. 4. The relation is likely universal for any binary liquid mixtures and also

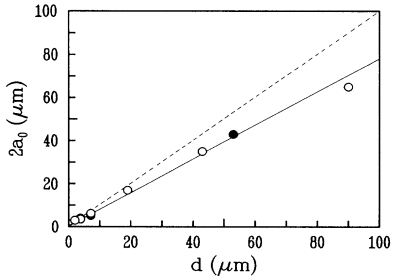

FIG. 4. Correlation between the initial diameter of a 2D disklike droplet ($2a_0$) and the thickness (d) for PVME/water (7/93) (○) and OCL/OS (3/7) (●) in 2D capillaries. The dashed line has a slope of 1 and the solid line is drawn to guide the eye.

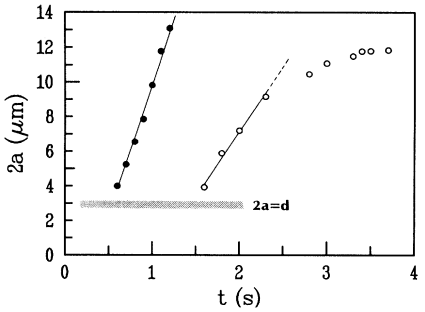

FIG. 5. Growth behavior of 2D disklike droplets for PVME/water (7/93) in a 2D capillary ($d \sim 3$ μm). Droplet diameter $2a$ is plotted against the phase-separation time t. ○: 33.3 °C; ●: 34.0 °C. In the shaded zone, $2a = d$.

for any quench conditions. The deviation from the relation $2a = d$ might be significant for a large d since the longitudinal curvature of the tube is not simply equal to $2/d$. However, the strong correlation between $2a_0$ and d observed experimentally supports the above discussion. With increasing d, the number of bridges (droplets) finally formed decreases. This can be explained by the fact that the condition $2a > d$ becomes more difficult to satisfy for a larger d since in a bicontinuous structure the number of percolated paths decreases with an increase in d and further bicontinuous tubes are spontaneously broken by any asymmetry during the coarsening.

In Fig. 5 the growth kinetics of the 2D disklike droplet is shown. Once the diameter $2a$ exceeds the thickness d, it grows linearly with time before the interaction between droplets starts to play a role. This linear growth behavior can be explained by the fact that the hydrodynamic flow from the wetting layer into the 2D disklike droplet is largely dominated by the pressure gradient coming from the longitudinal curvature $2/d$. In this approximation, $da/dt \propto (\sigma/\eta)g(d, d_w)$ where $g(d, d_w)$ is a function of d and the wetting layer thickness d_w, and a grows linearly with time. Figure 5 shows that regardless of the dynamics, the 2D disklike droplets always have the initial diameter of $2a_0 \sim d$. The difference in the slope is likely caused by the difference in σ as in Fig. 3. The difference in the time of $2a = d$ between 33.3 °C and 34.0 °C in Fig. 5 is likely due to the difference in the characteristic diffusion time ξ^2/D (ξ: the correlation length; $D = k_BT/5\pi\eta\xi$: the diffusion constant) between the two cases. The slowing down of the droplet growth observed in Fig. 5 is likely caused by the interdroplet interaction through the wetting layer. Since the wetting layer between neighboring droplets is finite, droplets cannot absorb the wetting layer independently in the late stage. In other words, $g(d, d_w)$ becomes a function of time through the change in d_w in this stage. In this final stage the droplets are attracted to each other by absorbing the wetting layers and also by the capillary instability of the tube formed between neighboring droplets [14].

In summary, we have found the universal wetting dynamics unique to a confined, symmetric mixture. It has also been demonstrated that the wetting layer formation in bicontinuous phase separation is strongly dependent on the spatial dimensionality of the geometrical constraint. The hydrodynamic coarsening unique to bicontinuous phase separation delocalizes the wetting effect and drastically accelerates the wetting dynamics. Thus the macroscopic wetting structure is formed within a short time. The phenomena described here should be universal for any binary mixtures. We actually observed the same phenomena in other mixtures such as polymer mixtures of polystyrene and PVME.

This work was partly supported by a Grant-in-Aid from the Ministry of Education, Science, and Culture, Japan, by a grant from Kanagawa Academy of Science and Technology, and by a grant from Toyota Physical and Chemical Research Institute.

[1] J.D. Gunton, M. San Miguel, and P. Sahni, in *Phase Transitions and Critical Phenomena,* edited by C. Domb and J.H. Lebowitz (Academic, London, 1983), Vol. 8.
[2] J.W. Cahn, J. Chem. Phys. **66,** 3667 (1977).
[3] D. Jasnow, Rep. Prog. Phys. **47,** 1059 (1984).
[4] P.G. de Gennes, Rev. Mod. Phys. **57,** 827 (1985).
[5] R. Moldover and J.W. Cahn, Science **207**, 1073 (1980).
[6] D.W. Pohl and W.I. Goldberg, Phys. Rev. Lett. **48**, 185 (1982).
[7] D. Beysens and D. Esteve, Phys. Rev. Lett. **54**, 2123 (1985).
[8] K. Williams and R.A. Dawe, J. Colloid Interface Sci. **117**, 81 (1987).
[9] A.J. Liu, D.J. Durian, E. Herbolzheimer, and S.A. Safran, Phys. Rev. Lett. **65**, 1897 (1990).
[10] P. Guenoun, D. Beysens, and M. Robert, Phys. Rev. Lett. **65**, 2406 (1990).
[11] P. Wiltzius and A. Cumming, Phys. Rev. Lett. **66**, 3000 (1991).
[12] F. Bruder and R. Brenn, Phys. Rev. Lett. **69,** 624 (1992).
[13] J. Bodensohn and W.I. Goldburg, Phys. Rev. A **46**, 5084 (1992).
[14] H. Tanaka, Phys. Rev. Lett. **70**, 53 (1993); (unpublished).
[15] E.D. Siggia, Phys. Rev. A **20**, 1979 (1979).

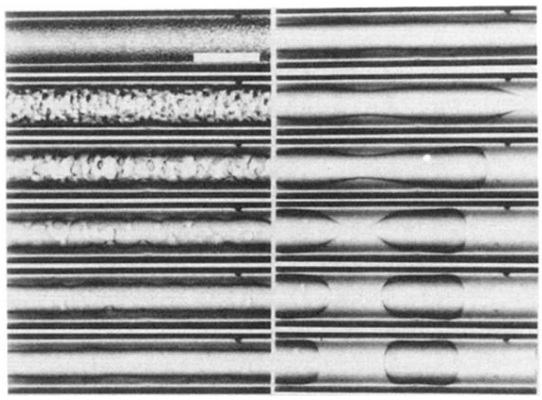

FIG. 1. Phase separation of PVME/water (7/93) in a 1D capillary. Photographs correspond to 0.5 s, 1.5 s, 2.5 s, 3.5 s, 4.5 s, 8.5 s (left column), 58.5 s, 148.5 s, 178.5 s, 238.5 s, 246.5 s, and 268.5 s (right column) from top to bottom, respectively, after the temperature jump from 32.5 °C to 33.3 °C. The bar is 200 μm in length.

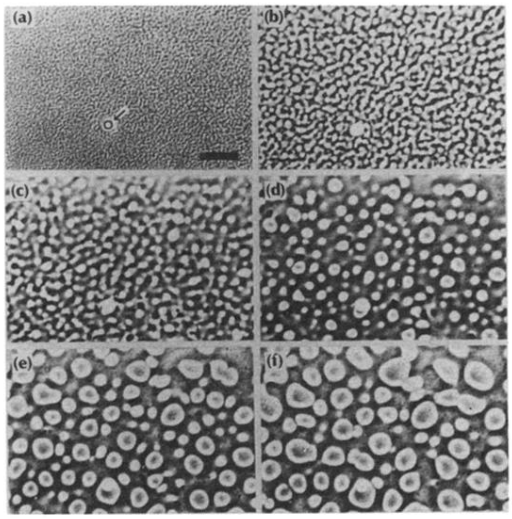

FIG. 2. Phase separation of PVME/water (7/93) in a 2D capillary ($d = 19$ μm). (a) 0.7 s, (b) 1.7 s, (c) 2.2 s, (d) 2.7 s, (e) 3.7 s, and (f) 4.7 s after the temperature jump from 32.8 °C to 33.7 °C. The arrow in (a) indicates the glass bead with the diameter of 19 μm. Its real size is also drawn in (a). The bar is 100 μm in length.